Actuators **2014**, *3*, 20-40; doi:10.3390/act3020020

OPEN ACCESS

actuators

ISSN 2076-0825

www.mdpi.com/journal/actuators

Article

A Two-Degree of Freedom Variable Stiffness Actuator Based on the MACCEPA Concept

Maarten Weckx *, Glenn Mathijssen, Idris Si Mhand Benali, Raphaël Furnemont, Ronald Van Ham, Dirk Lefeber and Bram Vanderborght

Department of Mechanical Engineering, Vrije Universiteit Brussel, Pleinlaan 2, Elsene 1050, Belgium; E-Mails: glenn.mathijssen@vub.ac.be (G.M.); Idris.Si.Mhand.Benali@vub.ac.be (I.S.M.B.); raphael.furnemont@ulb.ac.be (R.F.); Ronald.Van.Ham@vub.ac.be (R.V.H.); bram.vanderborght@vub.ac.be (B.M.)

* Author to whom correspondence should be addressed; E-Mail: maweckx@vub.ac.be; Tel.: +32-2-629-28-62.

Received: 30 December 2013; in revised form: 25 March 2014 / Accepted: 26 March 2014 / Published: 3 April 2014

Abstract: The current state-of-the-art of variable stiffness actuators consists mostly of different concepts for single-degree of freedom joints. However, in bio-inspired robotic applications, multiple degrees of freedom variable stiffness actuators are often desired. Currently, this is usually achieved by cascading single-degree of freedom actuators. The innovation presented in this work is a two-degree of freedom variable stiffness actuator using the mechanically adjustable and controllable equilibrium position actuator (MACCEPA) concept. The presented actuator is not a cascade of two single-degree of freedom actuators, but centralizes the two degrees of freedom in one single joint. Equilibrium position and stiffness of the actuator are, furthermore, independently controllable in both degrees of freedom. The design and experimental validation of the actuator are discussed in this work. The independence of adjusting the equilibrium position and stiffness of the actuator are experimentally validated. The results show that the measured characteristics of the actuator sufficiently match the theoretically calculated ones. Future work includes implementing the presented two-degree of freedom actuator in an application, like a bipedal robot or a robotic arm.

Keywords: compliant actuator; variable stiffness; two degrees of freedom; MACCEPA

---

1. Introduction

The versatile and dextrous nature of human movement is a result of the compliant single and multiple degrees of freedom joints in the body together with the adaptability of that compliance. Much research has been done towards adopting the principles of human actuation for robotic applications. The focus, however, is almost always on single-degree of freedom joints, while the human body possesses more multiple degrees of freedom joints than single-degree of freedom joints. In the following subsection, several human-inspired actuators are discussed. A more detailed description of the mechanically adjustable and controllable equilibrium position actuator (MACCEPA) follows, since the actuator presented in this work is a coupling of two MACCEPAs to achieve a two-degree of freedom actuator. The introduction will be concluded with the outline of this article.

1.1. Human-Inspired Actuation

Humans are capable of performing various complex tasks, show high dexterity and can adapt to dynamic environments. These characteristics are driven by the muscles as actuators. Since muscles can only exert force when they contract (isotonic contraction) or when their length remains unchanged (isometric contraction), an antagonistic setup of muscles is necessary for the bidirectional movement of joints. When either the agonist or the antagonist in such an antagonistic setup contracts, the angular position of the joint is changed. On the other hand, when both agonist and antagonist are tensioned equally, the position of the driven joint remains the same, but the stiffness of the joint is altered. Tensioning of both muscles increases joint stiffness, while relaxing of both muscles decreases joint stiffness. This mechanism allows the human body to regulate joint stiffness mechanically, rather than by force feedback. The ability of changing joint stiffness is, for instance, used to change walking speed [1], to change stride frequency during running [2] and to accommodate changes in surface stiffness [3].

Although many robots are designed to resemble humans and mimic their behavior, they are driven by stiff actuators, which do not possess the inherent compliance of muscle-driven human joints. Stiff actuators are based on the control paradigm of precise joint-angle control. They try to reach and maintain a desired position as fast as possible and regardless of the external forces, within the limits of the actuator. As a result, stiff actuators are energy inefficient and can easily cause damage to themselves and the environment when unexpected contact occurs. The concept of equilibrium position is introduced in compliant actuators, which possess a physical, elastic element capable of storing and releasing energy. The equilibrium position is the position in which the compliant actuator does not exert any force/torque. Furthermore, deviations from this position are allowed. This allows a safer human-robot interaction, shock absorbance and leads to a greater energy efficiency than stiff actuators [4]. Compliant actuators directly derived from human actuation are pneumatic artificial muscles (PAMs), which contract axially and expand radially when pressurized. PAMs have been successfully utilized in robotics for walking [5], running [6], jumping [7] and postural control [8]. The drawbacks of joints actuated with the antagonistic setup of PAMs are the nonlinear characteristics of the joint, the slow dynamics, the presence of hysteresis and the need for pressurized air [9]. The usage of electric motors in compliant actuator design can resolve these drawbacks. A well-known example is the series elastic actuator (SEA), consisting of a motor in series with a spring [10]. A straightforward

way of using electric motors is placing two SEA designs in an antagonistic setup. For the stiffness to be controllable, this type of setup needs non-linear springs [9]. This can be achieved by using physical non-linear springs [11,12] or by using mechanisms, containing linear springs, which have an overall non-linear stiffness characteristic [13–15]. The stiffness of a joint driven by such a setup is changed when the SEAs move in the same direction, while the equilibrium position is changed when they move in the opposite direction. This means that the control of the equilibrium position and stiffness is coupled, since the adaptation of both controllable parameters always requires the movement of both motors [4]. Other drawbacks are the size, extra complexity and the friction of the mechanisms acting as non-linear springs. The advantage of this compliant actuator design is that the stiffness characteristic of the overall system can be chosen during the design phase. Actuators based on the same principle, which allow for a decoupled equilibrium position and stiffness control, are the actuator with mechanically adjustable series compliance (AMASC) [16] or the continuous-state coupled elastic actuator (CCEA) [17], which still exhibit the drawback of complexity. An antagonistic setup is, however, not required to construct variable stiffness actuators. Examples are the actuator with variable stiffness and torque threshold (AVASTT) [18], the Actuator with Adjustable Stiffness-II (AwAS-II) [19], the VS-joint [20] and the mechanically adjustable compliance and controllable equilibrium position actuator (MACCEPA) [21]. These actuators all allow for independent equilibrium position and stiffness control [4,9].

Since humans posses multiple degrees of freedom joints, bio-inspired robotic applications often require multiple degrees of freedom actuators with variable stiffness. The three-dimensional shoulder and wrist joints of the human arm provide a large workspace and dexterity to the arms. During human locomotion, 23% of the total hip work is done in the frontal plane, while 74% of the total hip work is done in the sagittal plane [22]. The hip work in the frontal plane is done to support the body weight when the body mass is shifted laterally and to counteract a destabilizing gravitational moment in order to keep the pelvis and trunk erect [23]. One of the strategies the human body uses to cope with perturbations of the center of mass, particularly in the frontal plane, is widening the stance [24] by utilizing the frontal degrees of freedom in hips and ankles. These degrees of freedom, furthermore, allow for locomotion over surfaces inclined in the frontal plane and are used to adapt the gait when walking over irregular surfaces [25]. Because of the importance and use of multiple degrees of freedom joints in the human body, bio-inspired robotic applications often require multiple degrees of freedom actuators with variable stiffness. In cases where multiple degrees of freedom are wanted in one joint, however, cascades of single-degree of freedom actuators are usually used. The VSA-CubeBot is an example in which a robot's multiple degrees of freedom joints are formed by directly connecting variable stiffness actuators in series [26]. Another way to achieve this is by moving some parts of the actuator away from the joint, e.g., the motors, and using transmissions to drive the joint and/or change its stiffness [27,28]. The research on multiple degrees of freedom actuators with variable stiffness is still limited. One of the few examples is the multiple degrees of freedom actuator with variable stiffness based on two antagonistic setups of ANLESactuators [13]. This actuator has, however, the same disadvantages as other antagonistic setups previously mentioned. Additionally, the conceptual design of a three-degree of freedom variable stiffness actuator based on the MACCEPA concept is presented in [29]. This concept, however, has never

been built, nor tested. Different from variable stiffness actuators is the two-degree of freedom variable damping actuator, using electro-rheological fluids, proposed by Sakaguchi and Fukusho [30].

A novel concept of a two-degree of freedom variable stiffness actuator based on the MACCEPA is presented. The presented actuator is compact, centralizes both degrees of freedom in the joint and does not require additional transmissions other than the gearboxes of the motors to drive the equilibrium position and change the stiffness. Equilibrium position and stiffness can, furthermore, be controlled independently in both degrees of freedom, so the stiffness ellipse of the actuator can be adapted without influencing its equilibrium position.

1.2. MACCEPA

The MACCEPA [21] is a variable stiffness actuator, which allows for independent control of the equilibrium position and stiffness. As illustrated in Figure 1, it consists of three bodies, namely Link 1, Link 2 and the lever arm. Link 2 and the lever arm are connected through a linear tension spring. This spring can be pre-tensioned, thus giving an initial elongation, which will alter the MACCEPA's characteristics. Now, consider Link 1 as grounded. If the lever arm is aligned with Link 2, the force exerted by the spring (in case it is pre-tensioned) is aligned with Link 2. Therefore, no torque is exerted on Link 2. If the lever arm moves so that an angular deviation, α, between the lever arm and Link 2 arises, the force the spring exerts on Link 2 will not be aligned with Link 2 anymore. This results in a torque on Link 2, determined by the perpendicular component of the exerted force and the length, C, which tends to align Link 2 with the lever arm. The position of the lever arm, ϕ, is the equilibrium position of the MACCEPA, i.e., the position in which the actuator exerts no torque. By pre-tensioning the spring, thus giving it an initial elongation, the characteristics of the MACCEPA change and stiffness, which is the derivative of torque with respect to angle, of the actuator is altered. The torque-angle characteristic of the MACCEPA is given by:

$$T = kBCsin(\alpha)\left[1 + \frac{P - |B - C|}{\sqrt{B^2 + C^2 - 2BCcos(\alpha)}}\right] \tag{1}$$

with k the spring stiffness, P the pre-tension length, B the lever arm length and C the distance between the attachment point of the spring on Link 2 and the point of rotation. These parameters are indicated in Figure 1. Deriving this equation with respect to α yields the stiffness of the actuator. Equation (1) also shows that the parameters, B and C, are interchangeable. For ratios B/C or C/B bigger than five, the torque-angle characteristic of the MACCEPA is quasi-linear [21]. This allows for linearizing Equation (1). Consequently, for small angles α, the torque characteristic of the MACCEPA can be linearized as follows:

$$T = kBC\left(\frac{P}{|B - C|}\right)\alpha = \mu(P)\alpha \tag{2}$$

In this case, the MACCEPA acts as a torsional spring with a torsional spring stiffness, μ, linearly dependent on the pre-tension, P. As such, a motor that pre-tensions the spring enables one to change the joint stiffness, and a second motor that controls the lever arm can independently change the equilibrium position. A linear torque-angle characteristic is, however, not always desired. The human knee joint,

for instance, requires a stiffening characteristic for locomotion [31]. By replacing the lever arm of the MACCEPA by a profile disk, the characteristic of the actuator is changed dependent on the shape of the profile disk. This is the concept of the MACCEPA 2.0 [32].

The MACCEPA has been used in various applications, both inside the research lab as in other labs, e.g., bipedal walking robots [33,34], a jumping robot [32] and an ankle prosthesis [35]. Three of these applications are displayed in Figure 2.

Figure 1. The working principle and scheme of the mechanically adjustable and controllable equilibrium position actuator (MACCEPA) [21].

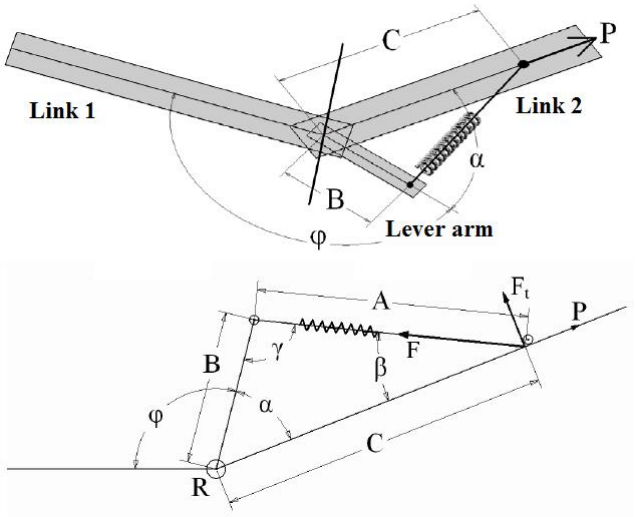

Figure 2. Applications using the MACCEPA: a bipedal walker (**a**) [33], a hopping robot (**b**) [32] and an ankle prosthesis (**c**) [35].

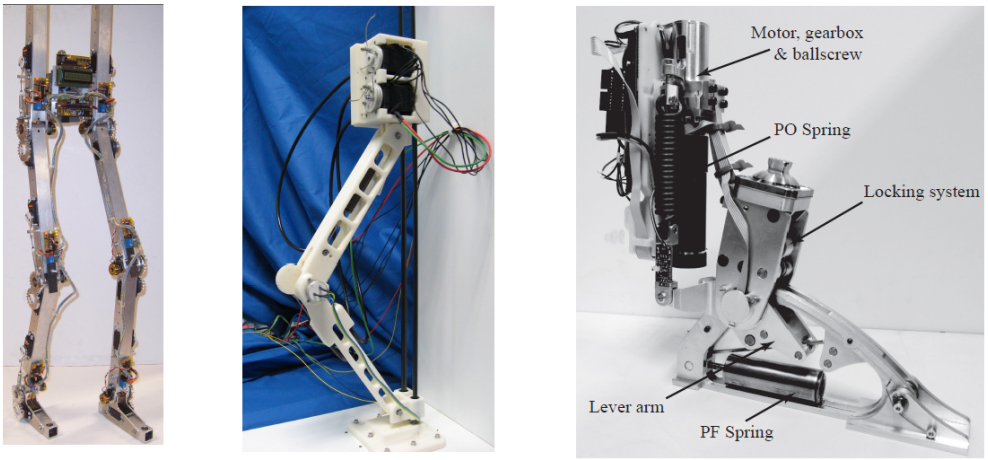

(a) **(b)** **(c)**

1.3. Outline

In Section 2, the design of the two-degree of freedom actuator will be discussed. This includes the mechanical design, assembly and electronics. Section 3 describes the experiments performed on the real

setup, which prove the independence of the equilibrium position and the stiffness of the actuator. A stiffness ellipse of the actuator is also experimentally composed in this section. Section 4 discusses the results of the experiments, and a conclusion is formulated in Section 5.

2. Design

In this section, the design of the two-degree of freedom MACCEPA, displayed in Figure 3, will be discussed. First, the concept of the presented actuator will be explained, followed by the mechanical design and construction of the parts of the actuator, with a focus on the central part located at the center of rotation. Subsequently, the chosen parameters for the MACCEPA structure in both degrees of freedom will be discussed together with the resulting actuator characteristics. This section will be concluded with a subsection on the sensors and electronics of the actuator.

Figure 3. CADdrawing of the presented two-degree of freedom MACCEPA.

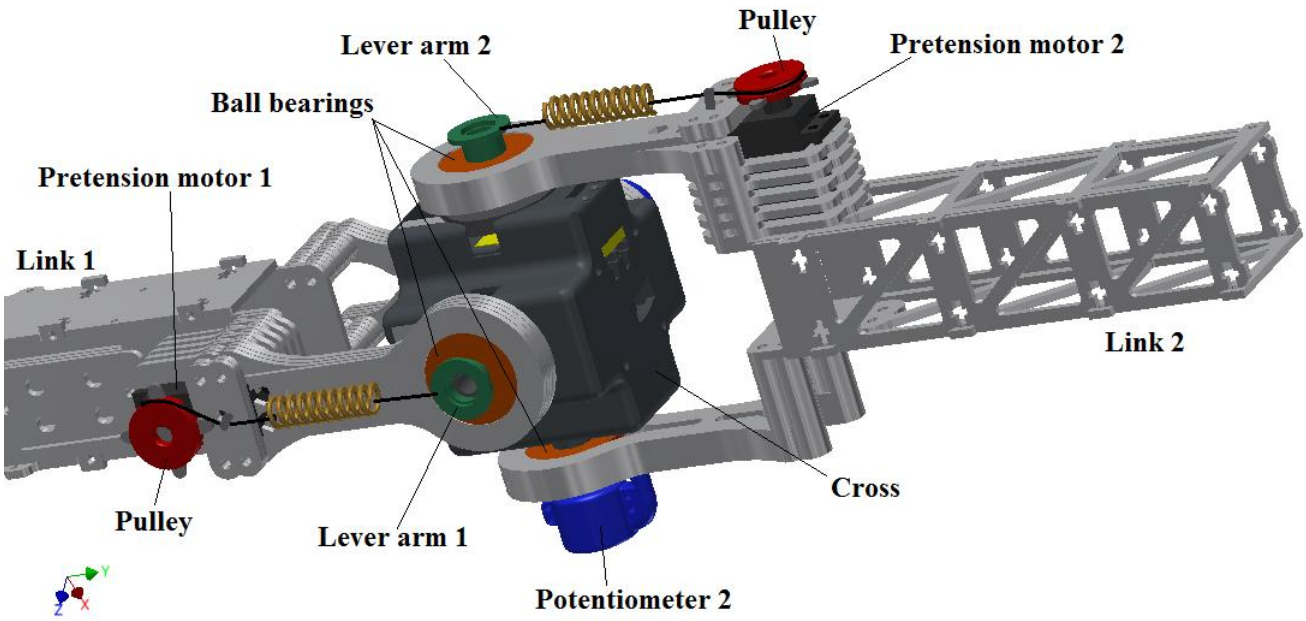

2.1. Concept

The joint, which connects both links, of a one degree of freedom MACCEPA has one axis of rotation. Its lever arm rotates around this same axis. The concept of the novel design starts from the universal joint with two orthogonal rotation axes to connect both links. The axes are indicated as Z_1 and Y_1 in Figure 4a. In this two degree of freedom case, the lever arm should be able to rotate around two orthogonal axes, which requires an additional universal joint with axes Z_2 and Y_2. The axes of both universal joints have to coincide to make the control of the equilibrium position and compliance independent. If the two axes of each rotation need to coincide, the four axes have to intersect in the same point. This results in a configuration of two Cardan joints inside one another, centered on the same point. The Cardan joint of the lever arm has to be actuated by two servomotors, to make the control of both equilibrium positions independent. The outer universal joint is used to connect Link 1 and Link 2.

The lever arm, to which the spring is connected, can now be rotated around two axes, relatively to the left body. The other end of the spring is connected to a pre-tension mechanism at Link 2, similar to the pre-tension mechanism of the one degree of freedom setup. With this setup, the equilibrium positions around both axes and the compliance can be controlled independently. Thus, each of the three actuators has its own function and does not interfere with the others.

Figure 4. MACCEPA with two degrees of freedom and one variable stiffness (**a**) and a complete MACCEPA with two degrees of freedom and two independent variable stiffnesses (**b**) [29].

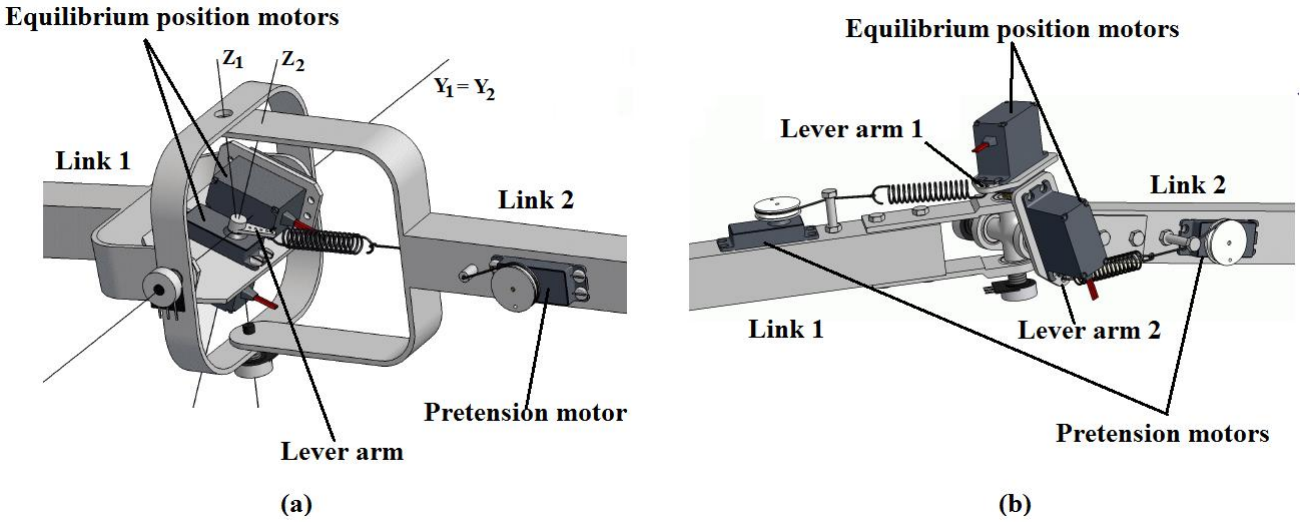

When the ability to control the stiffness in both degrees of freedom is required, a fourth motor has to be added. A setup with two rotational degrees of freedom for which the angle between the two intersecting axes is $90°$ is proposed. The links are connected by a universal joint, as is seen in Figure 4b. Concerning friction between the cables and mechanical structure, it is preferable that the motors that set the equilibrium positions and the pre-tension mechanisms are placed on different bodies. Since the pre-tension mechanisms need the most space, one is housed in each link, while the motors for the equilibrium positions are placed on the cross-shaped piece of the universal joint, as shown in Figure 4b. The shaft of the motor is connected to the cross-shaped part. The servomotors responsible for changing the equilibrium positions rotate relative to the cross-shaped piece and, thus, to the link in which their corresponding pre-tension mechanism is housed. A plate, acting as a lever arm, is placed on the servomotors. The result is a two-degree of freedom joint with four motors. Obviously, the actions of the four motors are completely independent. When one of the four parameters, one of the equilibrium positions or the compliance of one of the degrees of freedom has to be changed, only the corresponding servomotor has to be controlled.

A prototype based on the latter concept has been built and is presented in this work. To make the actuator more compact, the servomotors responsible for changing the equilibrium positions, by moving the lever arms, are placed inside the universal joint.

2.2. Mechanical Design

Figure 3 shows the design of the presented actuator. The actuator consists of three rigid bodies able to rotate with respect to each other. Two links are each connected to the cross-shaped piece of the universal joint, titling the cross. The cross houses the two servomotors driving the lever arms of both MACCEPAs and two angular position sensors measuring the relative position of the two links. The lever arms are connected to the corresponding pre-tension motors through cables and a linear spring. Each link houses one pre-tension motor; thus, half of each MACCEPA structure is housed in one of the links, while the other half is housed within the cross. A pulley is connected to the output of the pre-tension motors on which the spring is connected through a cable. To pre-tension the spring, an initial elongation is performed by winding up the cable on the pulley by rotating the pre-tension motor. Each MACCEPA is responsible for the movement in one degree of freedom; thus, the movement in both degrees of freedom is decoupled. When variable stiffness is not required along a degree of freedom, the corresponding pre-tension motor can be replaced by a fixed connection for the spring on the link, which will maintain the working principle of the MACCEPA.

Figure 5. Assembly of the cross.

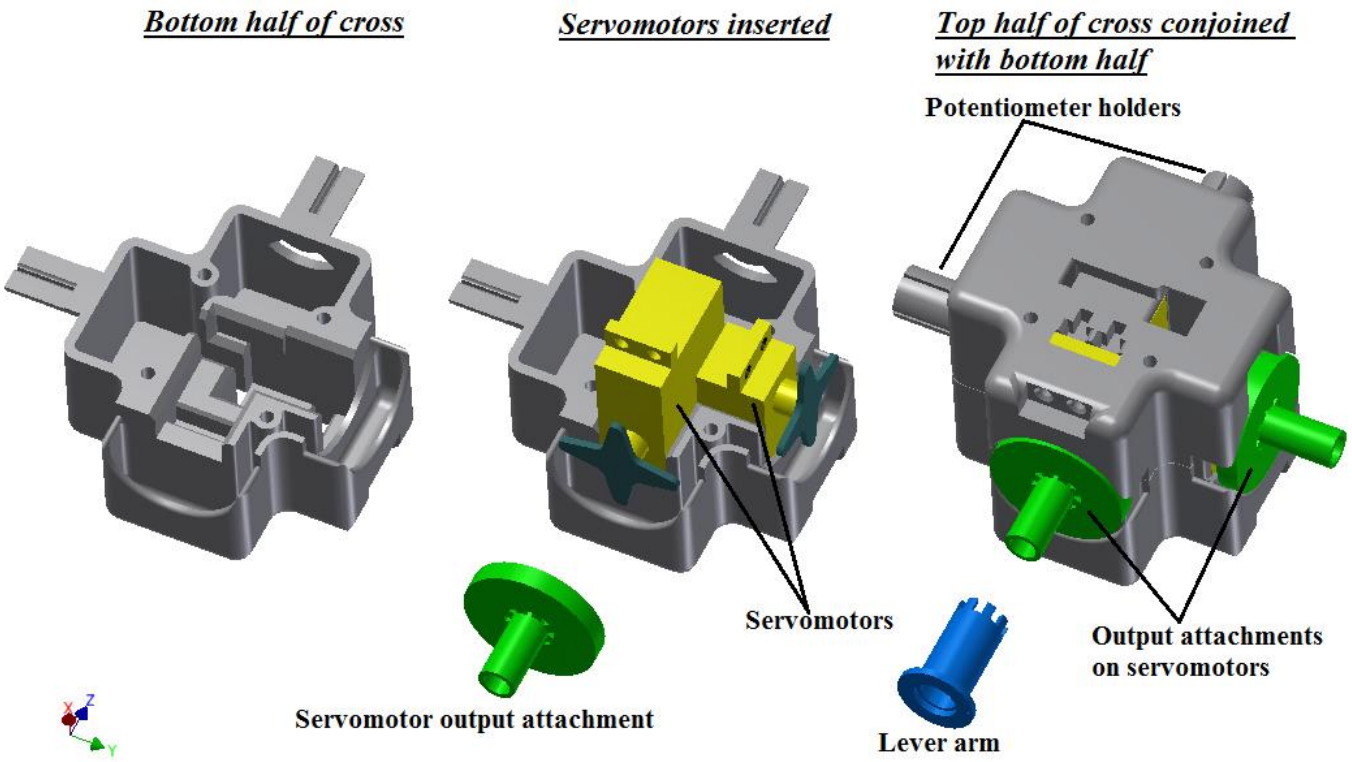

The cross' assembly is shown in Figure 5. The cross consists of two symmetric halves in which the servomotors driving the lever arms are placed. Before placing the servomotors inside the cross and the two halves of the cross are conjoined, an attachment is connected to the servomotor's output shaft. This is a disk with a shaft and is indicated as the "servomotor output attachment". Servomotors often come with a cross-shaped attachment on their output shaft. This allows the user to easily attach a part of choice onto the servomotor to act as the output. The servomotor output attachment allows one to easily assemble

the cross with the links to complete the assembly of the actuators. The lever arms are rings fixed to one end of a hollow shaft. This shaft is used to connect the lever arms to the corresponding servomotors. It is put through the ball bearings in the links and slid over the shaft of the servomotor output attachments. The hollow shafts of the lever arms end in pins with a particular cross-section, which fit in holes with the same cross-section in the disk of the servomotor output attachments, as shown in Figure 6. This fixes the lever arms to the servomotor's output shaft. In every degree of freedom, this is done on one side of the cross, while on the other side, a shaft is inherently part of the cross, indicated in Figure 5 as the potentiometer holders, which are put through the second ball bearing of the link, on the opposite side of the lever arm. The lever of a potentiometer is then fixed within the shaft, inherently part of the cross, while the housing of the potentiometer is fixed to the link. The potentiometer, thus, measures the angle between the cross and one link in the corresponding degree of freedom. This way, the links are connected to the cross.

Figure 6. The lever arm (blue) is slid over the servomotor output attachments (green) and connects through pins and holes of a particular shape.

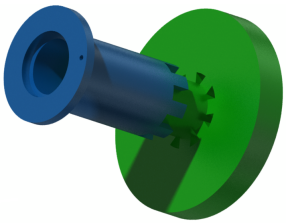

Figure 7. The two-degree of freedom MACCEPA.

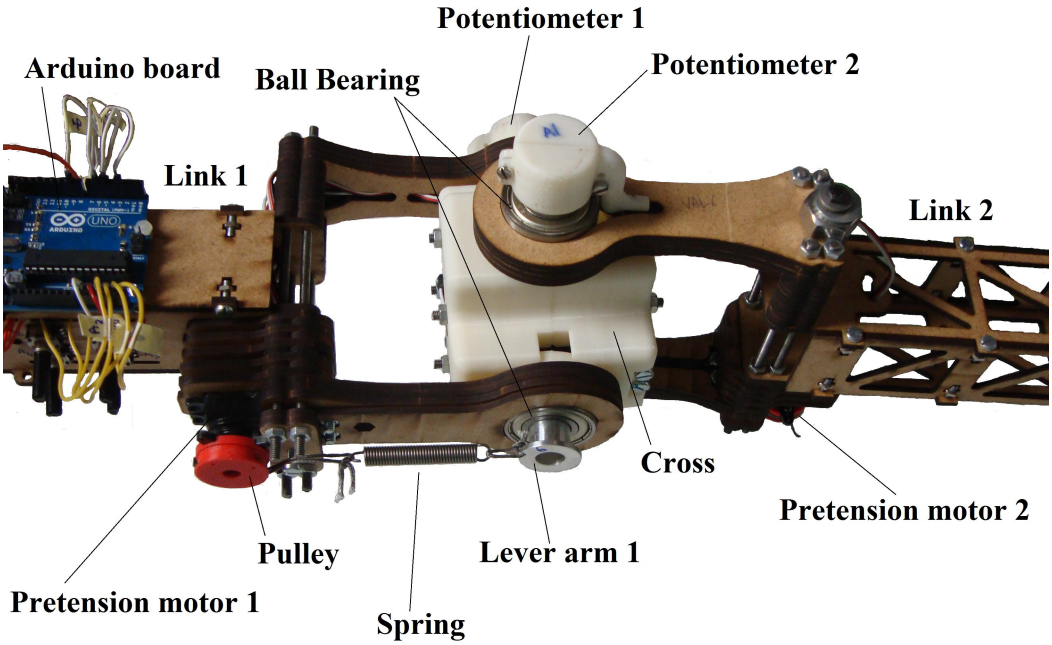

The lever arms are made out of aluminum. In the lever arms' ring, a hole is made, where one side of the spring is attached by means of a cable. The other side of the spring is connected to the pulley on the pre-tension motor housed in the corresponding link. The lever arm length, B, is thus the distance between this attachment point and the center point of the ring. The cross and the servomotor output attachments are all 3D-printed. The constructed actuator is shown in Figure 7.

2.3. MACCEPA Characteristics

The parameters of the MACCEPA structure in both degrees of freedom are chosen as the same. The parameters to be chosen, displayed in Figure 1, are lever arm length B, distance C from the axis of rotation to the attachment point of the spring and the spring constant, k.

To achieve a quasi-linear actuator, the C/B ratio has to be bigger than five, as previously mentioned. In this design, this ratio was chosen to be 9.5, and the value of C was set to 95 mm. Due to the fixed ratio, this results in a length of 10 mm for both lever arm's B. The used springs for both degrees of freedom have a spring constant of 1,180 N/m and a maximum elongation of 32.7 mm. The maximum pre-tension, P, is limited to 30 mm, so that at maximum pre-tension, a certain angle, α, is still allowed without deforming the springs. Figure 8 shows the elongation of the spring as a function of the deviation angle, α, for different pre-tensions. The red line represents the maximum allowed elongation of 32.7 mm of the chosen spring. At maximum pre-tension, the actuator, thus, still has a safe range of motion of approximately $40°$. The spring constant was chosen, so that the torque exerted by the MACCEPA at angles α larger than $30°$ for any allowed pre-tension would not exceed the stall torque of the servomotors driving the lever arms. This is out of precaution not to damage the servomotors at unexpected overloads.

Figure 8. The elongation of the spring as a function of deviation angle α for different pre-tension values and the maximum allowed elongation of the chosen spring.

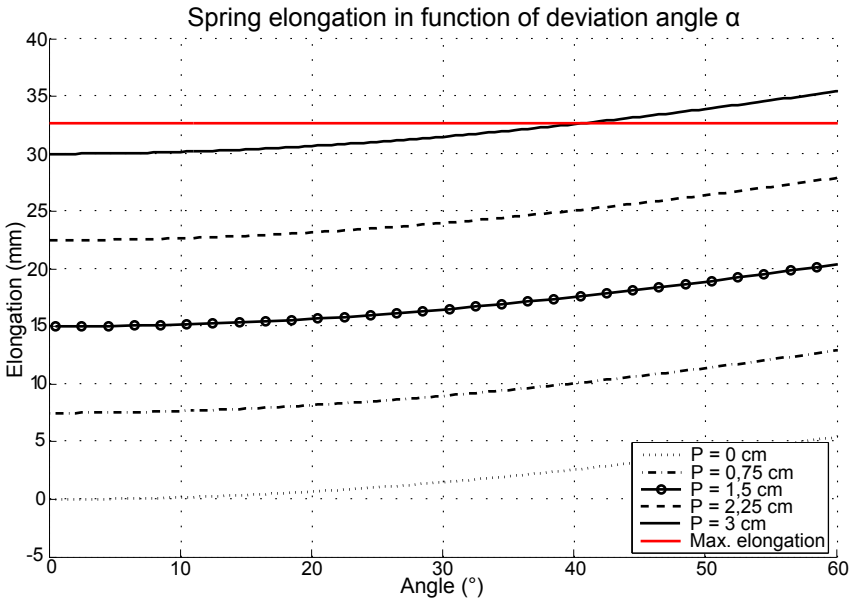

The resulting torque-angle characteristic of the actuators in both degrees of freedom for different pre-tensions is displayed in Figure 9a. The stiffness characteristic for different pre-tensions is displayed in Figure 9b. Note that the torque-angle characteristics are indeed quasi-linear and the corresponding stiffness characteristics constant for small angles α. At lower pre-tensions, this quasi-linearity is less outspoken, but as previously mentioned, a linear torque-angle characteristic is not always desired.

Figure 9. The torque-angle (**a**) and stiffness (**b**) characteristic of both MACCEPAs for different pre-tensions.

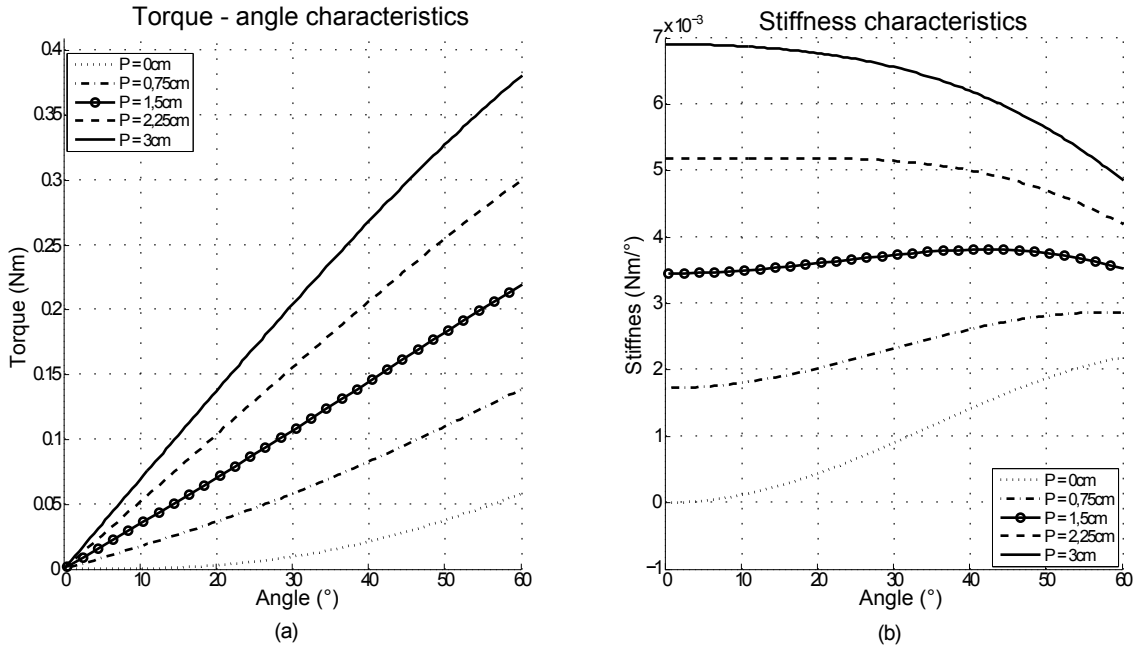

2.4. Electronics

The actuator has an on-board Arduino Uno microcontroller to read out the sensors, send appropriate commands to the four servomotors and exchange data with MATLAB scripts on an external computer for experimental purposes related to this work. Since the transmission between the spring and pre-tension motor is backdrivable, and the load on this motor has the same order of magnitude as the load on the equilibrium position motor, both motors are chosen as equal. All equilibrium position and pre-tension motors are Futaba s3003 servomotors, which have a stall torque of 0.41 Nm at 6 V.

As previously mentioned, two frictionless potentiometers are mounted, so that they measure the angle between the link and the cross in each degree of freedom. These measurements can be used, together with the knowledge of the equilibrium positions set by the servomotors driving the lever arms, to calculate the deviation angle, α, between the lever arm and link. The deviation angle, α, can be used to calculate the torque exerted by the actuator in one degree of freedom using Equation (1).

The Arduino Uno can be used to communicate with an external computer through its USBconnector. A MATLAB script is written to impose trajectories for the equilibrium positions and the pre-tensions. This script, furthermore, receives all sensor data collected by the Arduino Uno.

3. Experiments

In this section, the experiments on the real setup, displayed in Figure 7, and the results will be discussed. During the first experiment, it will be shown that the deviation angle of the actuator does not influence the actuator's characteristic and that only changing the stiffness, by changing the pre-tensions, alters the actuator's characteristic. The second set of experiments shows that changing the stiffness of the actuator does not influence the equilibrium position and *vice versa*. Finally, the stiffness ellipses of the actuator will be experimentally composed. All experiments are performed with the actuator suspended vertically and Link 1 grounded.

3.1. Experimental Torque-Angle Characteristics

In this experiment, the torque-angle characteristic of the MACCEPA in both degrees of freedom will be experimentally composed for different pre-tensions. The experiments will show that by changing the pre-tension of the MACCEPAs, the characteristics of the actuator are changed. These experiments will be alternately performed for both degrees of freedom.

Figure 10. Torques exerted by the MACCEPAs are measured by blocking the output link and using force sensors.

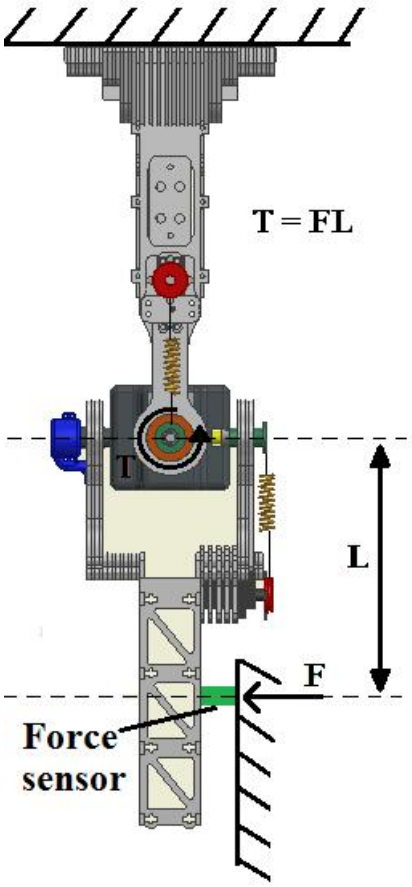

In order to measure the torque-angle characteristic of one degree of freedom of the actuator, the degree of freedom under test is blocked, while a force sensor is attached to output Link 2 between

this link and the blockage. The setup is illustrated in Figure 10. Since Link 2 is fixed in the vertical position by the blockage, the deviation angle, α, is equal to the equilibrium position. The equilibrium position of the MACCEPA is set to follow a predefined linear trajectory. This results in Link 2 pushing against the blockage and, thus, exerting a force, measured by the force sensor, which is related to the MACCEPA's exerted torque through the distance from the force sensor to the axis of rotation of the degree of freedom under test. Since the deviation angle, α, of the actuator is continuously changed during the experiments, performed with different pre-tensions, its relation with the actuator's stiffness can be investigated. Plotting the measured exerted torques against the deviation angle, α, which equals the predefined trajectory for the equilibrium position, yields the torque-angle characteristic of the MACCEPA in the degree of freedom under test for the set pre-tension. The measurements are performed alternately in both degrees of freedom for pre-tension values of 15.2 mm, 9.4 mm and 3.4 mm. The results are shown in Figure 11a,b, in which the blue curves represent the average of six measurements performed for the corresponding pre-tension in the corresponding degree of freedom, while the red curves represent the standard deviation from the average measurement.

Figure 11. The experimentally measured torque-angle (α) characteristics of DOF1 (**a**) and DOF 2 (**b**) compared with the theoretically calculated ones for three different pre-tensions. Red curves are the measurement deviations from the average measured blue curves.

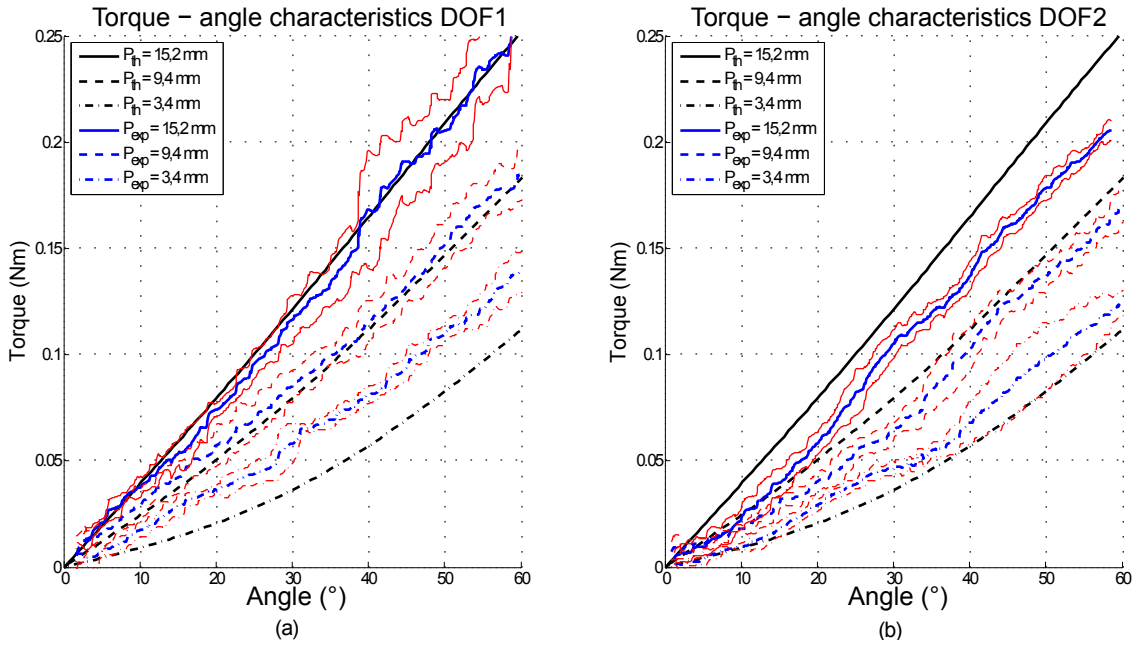

Figure 11a shows the results for degree of freedom 1, as defined in Figure 3. The experimental characteristics are observed to be quasi-linear, with linearity increasing for increasing pre-tension. The experimental characteristics, furthermore, match the theoretically calculated ones, calculated using Equation (1). There is a slight deviation of the experimental characteristic with a pre-tension of 3.4 mm from the corresponding theoretical one, however. It can be seen that between $\alpha = 30°$ and $\alpha = 60°$, the deviating experimental characteristic runs parallel with the corresponding theoretical characteristic, which means that despite the deviation, the stiffness of experimental and theoretical characteristics is the same in this region. Overall, the measured characteristics are not influenced by the continuously changing deviation

angle. Figure 11b shows the results for degree of freedom 2, as defined in Figure 3. Again, it is observed that different pre-tensions yield different torque-angle characteristics, and increasing the pre-tension increases the slope of the resulting characteristic, thus increases the stiffness of the actuator. In this degree of freedom, the increase in quasi-linearity with increasing pre-tension is less clearly observed from the experimental characteristics. The experimental characteristics for pre-tensions of 15.2 mm and 9.4 mm now deviate from the corresponding theoretical ones, calculated using Equation (1), in contrast to the results for degree of freedom 1. The experimental curve for a pre-tension of 3.4 mm deviates less from the corresponding theoretical one than for degree of freedom 1. The continuously changing deviation angle, furthermore, does not influence the overall stiffness of the characteristics. The measured torque curves in DOF2 are overall slightly lower than those in DOF 1. This can be explained by an angular deviation of Link 2 from the vertical position. Therefore, the force component parallel with the force sensor would have been bigger, and the measured perpendicular force would have been an underestimate of the force that was expected and observed during the experiments on DOF 1.

3.2. Independent Equilibrium Position and Stiffness

This experiment will show that the pre-tension and stiffness of the actuator does not influence the equilibrium position of the actuator and *vice versa*. The experiments will be performed for both degrees of freedom simultaneously.

Since the experiments are performed with the actuator suspended vertically, the static equilibrium of Link 2 will only coincide with the equilibrium position of the actuator if the equilibrium position is ($\phi_1 = 0°$, $\phi_2 = 0°$), thus the most downward position of the lever arms. As a result of the weight of Link 2 under the influence of gravity and the allowed deviation from the equilibrium position, inherent to compliant actuators, Link 2 will deviate from the equilibrium position for any other setting. For the experiment, the equilibrium position of the actuator will be set to a predefined value, as will the pre-tensions in both degrees of freedom. Link 2 is arbitrarily pulled out of its static equilibrium, i.e., its initial position, and released. This induces a passive, two-dimensional oscillation back to the initial position driven by the torques exerted by the actuator that tend to align the link with the equilibrium position. During the experiment, the angular position of the link will be measured by the potentiometers along the two degrees of freedom. Performing this experiment with different pre-tensions in both degrees of freedom will show that regardless of the stiffness of the actuator, the link will return to its initial position. Repeating these measurements for different equilibrium positions will yield the same conclusion. The experiment is performed for equilibrium positions ($\phi_1 = 0°$, $\phi_2 = 0°$) and ($\phi_1 = 52°$, $\phi_2 = 47°$). The experiment for each equilibrium position is performed with three different pre-tensions, set equally for both degrees of freedom.

The results of the experiment with the equilibrium position set to ($\phi_1 = 0°$, $\phi_2 = 0°$) and for three different pre-tensions, equal for both degrees of freedom, is shown in Figure 12. It shows the oscillations of Link 2 in both degrees of freedom separately. A 3D graph is furthermore given of the two-dimensional oscillation, by combining the separate one-dimensional measurements, in time, and shows how Link 2 spirals back to its initial position. Here, the initial position of Link 2 is equal to the set equilibrium

position. It can be seen that regardless of the pre-tension value, Link 2 returns to its initial position, i.e., the equilibrium position of the actuator in this case. The equilibrium position remains unchanged. The results of the experiment with the equilibrium position set to ($\phi_1 = 52°$, $\phi_2 = 47°$) and for three different pre-tensions, equal for both degrees of freedom, is shown in Figure 13. It shows the same graphs as Figure 12. Here, the initial position of Link 2 is, however, not the same as the set equilibrium position, for reasons previously mentioned. The initial position is now dependent on the pre-tension. Different pre-tensions yield different torque-angle characteristics of the actuator, and thus, the torque necessary to compensate the gravitational torque acting on Link 2 is exerted at different deviation angles α depending on the pre-tension. The changing initial position under influence of pre-tension can be clearly seen. Additionally, it shows that again Link 2 returns to its initial position regardless of the set pre-tension, and the equilibrium position remains unchanged regardless of the set pre-tension.

Figure 12. Induced passive oscillations for equilibrium position ($\phi_1 = 0°$, $\phi_2 = 0°$) at different pre-tensions.

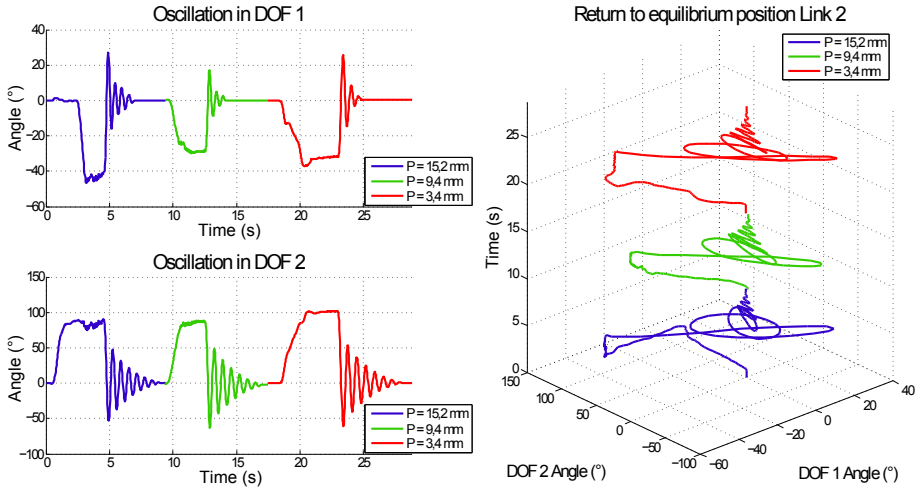

Figure 13. Induced passive oscillations for equilibrium position ($\phi_1 = 52°$, $\phi_2 = 47°$) at different pre-tensions.

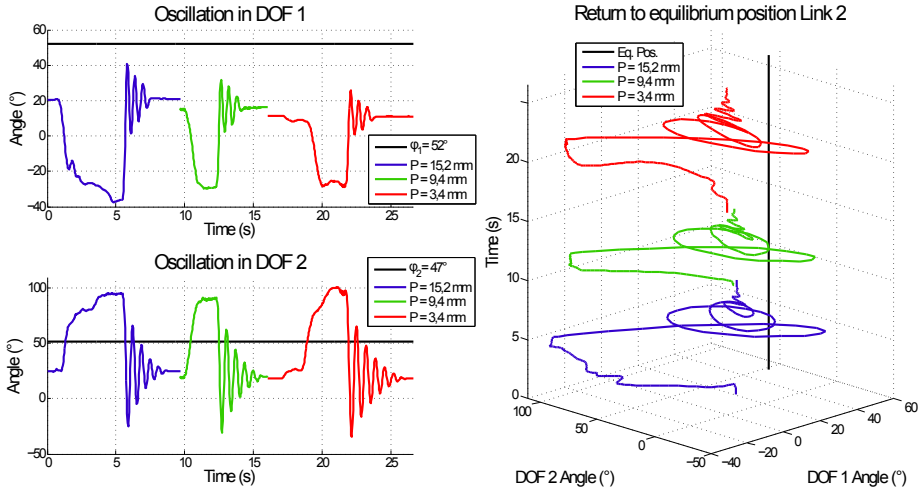

3.3. The Stiffness Ellipse Experimentally Composed

In this section, the stiffness ellipse of the actuator will be experimentally composed. The results will be compared to the corresponding theoretically composed stiffness ellipse.

The stiffness of a two-dimensional joint is represented by the stiffness matrix, which provides the relation between torque and angular displacement:

$$\begin{bmatrix} T_x \\ T_y \end{bmatrix} = \begin{bmatrix} K_{xx} & K_{xy} \\ K_{yx} & K_{yy} \end{bmatrix} \begin{bmatrix} d\alpha_x \\ d\alpha_y \end{bmatrix} \tag{3}$$

where T_x and T_y are the restoring torques to counteract the imposed angular displacements, $d\alpha_x$ and $d\alpha_y$. K_{fg} are the elements of the stiffness matrix, which provide the relation between the angular displacement and resulting restoring torques. The stiffness matrix can be represented geometrically by multiplying it with a rotational angular displacement of unit amplitude [36], e.g.,:

$$\begin{bmatrix} d\alpha_x \\ d\alpha_y \end{bmatrix} = \begin{bmatrix} \cos t \\ \sin t \end{bmatrix} \qquad 0 \leq t \leq 2\pi \tag{4}$$

The resulting stiffness ellipse shows the predicted restoring torque in each direction for an angular displacement of unit amplitude. The major axis indicates the direction and magnitude of maximal joint stiffness, while the minor axis indicates the direction and magnitude of least joint stiffness. In order to construct the theoretical stiffness ellipse of the two-degree of freedom MACCEPA μ(P), Equation (2) is used to approximate the diagonal elements of the stiffness matrix. Since the MACCEPAs in both degrees of freedom are decoupled, the non-diagonal elements of the stiffness matrix are zero, thus $K_{xy} = K_{yx} = 0$. Using Equation (2) is justified, since the stiffness ellipse is constructed for angular displacements of unit amplitude and the MACCEPA is quasi-linear for small deviations from the equilibrium position. In case of the two degrees of freedom MACCEPA with variable compliance, an infinite amount of stiffness ellipses can be constructed for different values for the pre-tensions within their possible range. As a result of the identical design of the MACCEPA for both degrees of freedom, setting identical pre-tensions for the degrees of freedom yields circles instead of ellipses. The x- and y-direction of the actuator correspond respectively with DOF 1 and DOF 2, as defined previously. The indices, x and y, will, therefore, be replaced by the indices, 1 and 2, hereafter.

In order to construct the stiffness ellipse experimentally, the actuator remains suspended vertically, and the equilibrium position of both degrees of freedom is fixed at 0°. The torque exerted by the actuator is measured as is done for the experiments described in Section 3.1. Since the stiffness ellipse is measured in two dimensions, both degrees of freedom of the actuator are blocked, as illustrated in Figure 10; so, two force sensors are used to determine the exerted torque in the corresponding directions. The lever arms of the MACCEPAs are moved along predefined trajectories, thus continuously changing the equilibrium position of the actuator. In this setup, the equilibrium position of the actuator equals the deviation angles, α_1 and α_2. The exerted torques are continuously measured. If the predefined trajectory for the actuator's equilibrium position contains n points, then the measurements yield n measurement points, (α_{1i}, α_{2i}) being the displacement angles and (T_{1i}, T_{2i}) the restoring torques, due to the corresponding angular displacement. These measurement points are used to numerically calculate

the elements, K_{fg}, of the stiffness matrix by means of a linear least squares method. Using Equation (3), a cost function can be composed to be minimized by the linear least squares method:

$$E_i = \begin{bmatrix} T_{xi} \\ T_{yi} \end{bmatrix} - \begin{bmatrix} K_{11} & K_{12} \\ K_{21} & K_{22} \end{bmatrix} \begin{bmatrix} \alpha_{1i} \\ \alpha_{2i} \end{bmatrix} \tag{5}$$

So that the error for measurement i becomes:

$$\epsilon_i = \frac{1}{2} E_i^T E_i \tag{6}$$

and the cost function is defined as:

$$\epsilon = \sum_{i=1}^{n} \epsilon_i \tag{7}$$

The stiffness ellipse of the actuator will be experimentally constructed for the following set of pre-tensions: (P_1 = 9.4 mm, P_2 = 9.4 mm).

Figure 14. The measured and theoretical stiffness ellipses of the two-degree of freedom MACCEPA for pre-tension set (P_1 = 9.4 mm, P_2 = 9.4 mm).

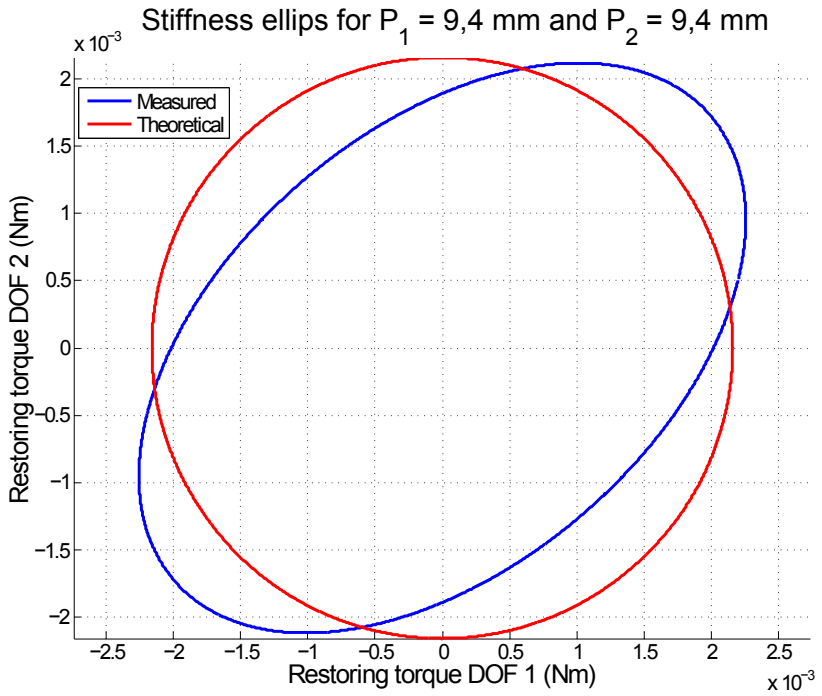

In Figure 14, the measured stiffness ellipse is compared with the theoretically calculated one for the chosen set of pre-tensions. The corresponding experimentally determined and theoretically calculated stiffness matrices are listed in Table 1. The measured ellipse should be a circle in this case. A tilted ellipse is, however, observed. The tilt angle of the ellipse is a result of non-zero non-diagonal elements of the stiffness matrix, as can be seen in Table 1. This implies that a deviation from the equilibrium position in one degree of freedom of the actuator results in torques exerted in both degrees of freedom. This is not correct, since both MACCEPA structures of the presented actuator are separated and their operation is decoupled. This can be explained by forces parallel to the force sensors, due to friction or

small deviations of Link 2 from the vertical position. This results in undesired force components in one degree of freedom, while force is exerted in the other degree of freedom. The diagonal elements of the experimentally composed stiffness ellipse do match those of the theoretically calculated ones.

Table 1. The experimentally determined and theoretically calculated stiffness matrices corresponding to Figure 14.

$K_{measured}$ (Nm/°)		$K_{theoretical}$ (Nm/°)	
0.0022	0.0005	0.0022	0
0.0005	0.0021	0	0.0022

4. Results

In this section, the results of the experiments, discussed in Section 3, performed on the presented two-degree of freedom actuator, will be summarized.

It has been shown that the equilibrium position and stiffness of the presented actuator can be changed independently. Changing the pre-tension of the MACCEPA in one degree of freedom of the actuator will change the torque-angle characteristic and stiffness characteristic of this degree of freedom without influencing the equilibrium position of the actuator. *Vice versa*, changing the equilibrium position does not influence the stiffness of the actuator. The static equilibrium, relative to the equilibrium position, of the output link of the actuator is dependent on the plane in which the actuator is placed, the actuator's equilibrium position, and the mass of the output link. The characteristics of both degrees of freedom can furthermore be changed independently. The range of stiffness characteristics is determined by the maximum allowed elongation of the springs used in the MACCEPA design. The measured torque-angle characteristics match the theoretically calculated ones of the actuator. The stiffness, thus, also matches the theoretical stiffness. As a result, the stiffness ellipse of representing the stiffness matrix of the actuator joint can be changed by changing the pre-tension in the degrees of freedom.

5. Conclusions

A novel two-degree of freedom variable stiffness actuator based on the MACCEPA concept is presented in this work. The actuator offers a solution for bio-inspired robotic applications, which require multiple degrees of freedom actuators with variable stiffness. The actuator is compact, centralizes both degrees of freedom in the joint and does not require additional transmissions, other than the gearboxes of the motors, to drive the equilibrium position and change the stiffness. Equilibrium position and stiffness can, furthermore, be controlled independently in both degrees of freedom; so, the stiffness ellipse of the actuator can be adapted without influencing its equilibrium position. Future work includes implementing the novel two-degree of freedom actuator in a humanoid walking robot or a robotic arm.

Acknowledgments

This work has been funded by the European Commission 7th Framework Program as part of the project, H2R(No. 600698).

Author Contributions

Maarten Weckx is the main author of the article. He is responsible for the design and realization of the presented research. Maarten Weckx and Glenn Mathijssen conducted the experiments. Idris Si Mhand Benali is responsible for developing the mechanical design. Raphaël Furnemont contributed to the mechatronic design. Ronald Van Ham is responsible for the first 1 DOF and 2 DOF MACCEPA concepts. Dirk Lefeber and Bram Vanderborght supervised the project and helped finalize the article.

Conflicts of Interest

The authors declare no conflicts of interest.

References

1. Seyoung, K.; Sukyung, P. Leg stiffness increases with speed to modulate gait frequency and propulsion energy. *J. Biomech.* **2011**, *44*, 1253–1258.
2. Farley, C.; Gonzalez, O. Leg stiffness and stride frequency in human running. *J. Biomech.* **1996**, *29*, 181–186.
3. Ferris, D.; Louie, M.; Farley, C. Running in the real world: Adjusting leg stiffness for different surfaces. In Proceedings of the Royal Society of London B: Biological Sciences: London, United Kingdom, 1998, Volume 265, pp. 989–994.
4. Vanderborght, B.; Albu-Schaeffer, A.; Bicchi, A.; Caldwell, D.; Tsagarakis, N.; van Damme, M.; Lefeber, D.; van Ham, R.; Jafari, A.; Burdet, E.; *et al*. Variable impedance actuators: A review. *Rob. Autonom. Syst.* **2013**, *61*, 1601–1614.
5. Vanderborght, B.; van Ham, R.; Verrelst, B.; van Damme, M.; Lefeber, D. Overview of the lucy project: Dynamic stabilization of a biped powered by pneumatic artificial muscles. *Adv. Rob.* **2008**, *22*, 1027–1051.
6. Hosoda, K.; Takuma, T.; Nakamoto, A. Design and control of 2D biped that can walk and run with pneumatic artificial muscles. In Proceedings of the IEEE 2006 6th IEEE-RAS International Conference on Humanoid Robots, 2006; pp. 284–289.
7. Niiyama, R.; Nagakubo, A.; Kuniyoshi, Y. Mowgli: A bipedal jumping and landing robot with an artificial musculoskeletal system. In Proceedings of the 2007 IEEE International Conference on Robotics and Automation, 2007; pp. 2546–2551.
8. Hettich, G.; Fennell, L.; Mergner, T. Double inverted pendulum model of reactive human stance control. *Multibody Dyn.* **2011**.
9. Van Ham, R.; Sugar, T.; Vanderborght, B.; Hollander, K.; Lefeber, D. Compliant actuator designs. *IEEE Rob. Autom. Mag.* **2009**, *16*, 81–94.

10. Pratt, G.A.; Williamson, M.M. Series elastic actuators. In Proceedings of the IEEE/RSJ Human Robot Interaction and Cooperative Robots, 1995; Volume 1, pp. 399–406.
11. English, C.; Russell, D. Mechanics and stiffness limitations of a variable stiffness actuator for use in prosthetic limbs. *Mech. Mach. Theory* **1999**, *34*, 7–25.
12. Nam, K.H.; Kim, B.S.; Song, J.B. Compliant actuation of parallel-type variable stiffness actuator based on antagonistic actuation. *J. Mech. Sci. Technol.* **2010**, *24*, 2315–2321.
13. Koganezawa, K.; Nakazawa, T.; Inaba, T. Antagonistic control of multi-DOF joint by using the actuator with non-linear elasticity. In Proceedings of the 2006 IEEE International Conference on Robotics and Automation, 15-19 May 2006; pp. 2201–2207.
14. Migliore, S.; Brown, E.; deWeerth, S. Biologically inspired joint stiffness control. In Proceedings of the 2005 IEEE International Conference on Robotics and Automation (ICRA), 18-22 April 2005; pp. 4508–4513.
15. Tonietti, G.; Schiavi, R.; Bicchi, A. Design and control of a variable stiffness actuator for safe and fast physical human/robot interaction. In Proceedings of the 2005 IEEE International Conference on Robotics and Automation (ICRA), 2005; pp. 526–531.
16. Hurst, J. Chestnutt, J.E.; Rizzi, A.A. The Actuator With Mechanically Adjustable Series Compliance. *IEEE Trans. Robot.* **2010**, *26*, 597–606.
17. Huang, T.H.; Kuan, J.Y.; Huang, H.P. Design of a new variable stiffness actuator and application for assistive exercise control. In Proceedings of the 2011 IEEE/RSJ International Conference on Intelligent Robots and Systems (IROS), 25-30 September 2011; pp. 372–377.
18. Martínez, J.L.; Blanco, J.; Vallejo, D.G.; Torres, J.; Fernández, A.G. AVASTT: A New Variable Stiffness Actuator with Torque Threshold. ROBOT2013: First Iberian Robotics Conference. Springer, 2014, pp. 573–583.
19. Jafari, A.; Tsagarakis, N.; Sardellitti, I.; Caldwell, D. A new actuator with adjustable stiffness based on a variable ratio lever mechanism. *IEEE/ASME Trans. Mechatron.* **2012**, *19*, 1–9.
20. Wolf, S.; Hirzinger, G. A new variable stiffness design: Matching requirements of the next robot generation. In Proceedings of the 2008 IEEE International Conference on Robotics and Automation, 19-23 May 2008; pp. 1741–1746.
21. Van Ham, R.; vanderborght, B.; van Damme, M.; Verrelst, B.; Lefeber, D. MACCEPA, the mechanically adjustable compliance and controllable equilibrium position actuator: Design and implementation in a biped robot. *Rob. Autonom. Syst.* **2007**, *55*, 761–768.
22. Eng, J.; Winter, D. Kinetic analysis of the lower limbs during walking: what information can be gained from a three-dimensional model? *J. Biomech.* **1995**, *28*, 753–758.
23. MacKinnon, C.; Winter, D. Control of whole body balance in the frontal plane during human walking. *J. Biomech.* **1993**, *26*, 633–644.
24. Goodworth, A.; Peterka, R. Influence of stance width on frontal plane postural dynamics and coordination in human balance control. *J. Neurophysiol.* **2010**, *2*, 1103–1118.
25. Manz, H.; lord, S.; Fitzpatrick, R. Acceleration pattern of the head and pelvis when walking on level and irregular surfaces. *Gait Post.* **2003**, *18*, 35–46.

26. Catalano, M.; Grioli, G.; Garabini, M.; Bonomo, F.; Mancinit, M.; Tsagarakis, N.; Bicchi, A. VSA-CubeBot: A modular variable stiffness platform for multiple degrees of freedom robots. In Proceedings of the 2011 IEEE International Conference on Robotics and Automation (ICRA), 9-13 May 2011; pp. 5090–5095.
27. Hobbelen, D.; de Boer, T.; Wisse, M. System overview of bipedal robots flame and tulip: Tailor-made for limit cycle walking. In Proceedings of the IEEE/RSJ International Conference on Intelligent Robots and Systems, 22-26 September 2008; pp. 2486–2491.
28. Gallego, J.; Forner-Cordero, A.; Moreno, J.; Montellano, A.; Turewska, E.; Pons, J. Continuous assesment of gait stability in limit cycle walkers. In Proceedings of the 2010 3rd IEEE/RAS and EMBS International Conference on Biomedical Robotics and Biomechanics (BioRob), 26-29 September 2010; pp. 734–739.
29. Van Ham, R.; van Damme, M.; Verrelst, B.; Vanderborght, B.; Lefeber, D. MACCEPA, the mechanically adjustable compliance and controllable equilibrium position actuator: A 3 DOF joint with two independent compliances. *Int. Appl. Mech.* **2007**, *43*, 467–474.
30. Sakaguchi, M.; Furusho, J. Development of high-performance actuators using ER fluids. *J. Intell. Mater. Syst. Struct.* **1999**, *10*, 666–670.
31. Seyfarth, A.; Geyer, H.; Blickhan, S.; Lipfert, S.; Rummel, J.; Minekawa, Y.; Iida, F. Running and Walking With Compliant Legs. In *Fast Motions in Biomechanics and Robotics*; Springer: Berlin, Germany, 2006; pp. 383–401.
32. Vanderborght, B.; Tsagarakis, N.; van Ham, R.; Thorson, I.; Caldwell, D. MACCEPA 2.0: Compliant actuator used for energy efficient hopping robot chobino 1D. *Autonom. Rob.* **2011**, *31*, 55–65.
33. Huang, Y.; Vanderborght, B.; van Ham, R.; Wang, Q.; van Damme, M.; Guangming, X.; Lefeber, D. Step length and velocity control of dynamic bipedal walking robot with adaptable compliant joints. *IEEE/ASME Trans. Mechatron.* **2013**, *18*, 598–611.
34. Mao, Y.; Wang, J.; Jia, P.; Li, S.; Qiu, Z.; Zhang, L.; Han, Z. A reinforcement learning based dynamic walking control. In Proceedings of the IEEE International Conference on Robotics and Automation, 10-14 April 2007; pp. 3609–3614.
35. Cherelle, P.; Grosu, V.; Matthys, A.; Vanderborght, B.; Lefeber, D. Design and validation of the ankle mimicing prosthetic (AMP-) foot 2.0. *IEEE Trans. Neur. Syst. Rehabil. Eng.* **2013**, *22*, 1.
36. Mussa-Ivaldi, F.; Hogan, N.; Bizzi, E. Neural, mechanical, and geometric factors subserving arm posture in humans. *J. Neurosci.* **1985**, *5*, 2732–2743.